

Elastic scattering of ${}^9\text{Be} + {}^{80}\text{Se}$ and the breakup threshold anomaly

Daniel Abriola¹, Fernando Gollan^{1,2}, Andrés Arazi^{1,2}, Guillermo V. Martí¹, and Jorge E. Testoni¹

¹Laboratorio TANDAR, Gerencia de Investigación y Aplicaciones, Departamento de Física Experimental, Comisión Nacional de Energía Atómica, B1650KNA, San Martín, Buenos Aires, Argentina

²CONICET, Av. Rivadavia 1917, C1033AAJ Buenos Aires, Argentina

abriola@tandar.cnea.gov.ar

Abstract

We study the threshold anomaly displayed in the energy dependence of optical potentials describing elastic-scattering angular distributions of weakly bound nuclei with three different models: a) a semi-microscopic double folding potential with two free parameters, b) a phenomenological Wood-Saxon potential with six free parameters and c) an exponential potential with two free parameters. In this kind of nuclei, the coupling to the breakup channel is reflected as an increasing of the imaginary part of the potential as the bombarding energy decreases below the Coulomb barrier, while the real part of the potential (linked to the imaginary part by the dispersion relation) decreases in strength. This behavior is called breakup threshold anomaly (BTA).

In this work, we apply this analysis to experimental data for the elastic scattering in the ${}^9\text{Be} + {}^{80}\text{Se}$ system at eleven bombarding energies around the Coulomb barrier, obtained at the 20 MV tandem accelerator of the TANDAR Laboratory at Buenos Aires. Using the covariance-matrix method to estimate the uncertainties, the presence of the BTA in this system is unambiguously determined, independently of the model chosen for the nuclear potential.

Key words: elastic scattering; optical models; energy dependence; beryllium 9; selenium 80; threshold energy

Dispersión elástica de ${}^9\text{Be} + {}^{80}\text{Se}$ y la anomalía de umbral de ruptura

Resumen

Estudiamos la anomalía de umbral presente en la dependencia con la energía de potenciales ópticos que describen la dispersión elástica de núcleos débilmente ligados, usando tres tipos de potenciales ópticos para la descripción de las distribuciones angulares: a) un potencial semimicroscópico doblemente plegado con dos parámetros libres, b) un potencial fenomenológico tipo Wood-Saxon con seis parámetros libres y c) un potencial exponencial con dos parámetros libres. En este tipo de núcleos, el acoplamiento al canal de ruptura se refleja como un aumento de la parte imaginaria del potencial al decrecer la energía de bombardeo por debajo de la barrera de Coulomb, mientras que la parte real (vinculada a la parte imaginaria por la relación de dispersión) disminuye en intensidad. Este comportamiento se denomina anomalía de umbral de ruptura (BTA).

En el presente trabajo, se aplica este análisis a datos experimentales concernientes a la dispersión elástica en el sistema ${}^9\text{Be} + {}^{80}\text{Se}$ a 11 energías de bombardeo alrededor de la barrera de Coulomb, obtenidos con el acelerador de 20MV del Laboratorio TANDAR en Buenos Aires. Se utilizó el método de matriz de covarianza para estimar las incertidumbres, se determina inequívocamente la presencia de la BTA en este sistema, independientemente del modelo elegido para el potencial nuclear.

Palabras clave: dispersión elástica; modelos ópticos; dependencia energética; berilio 9; selenio 80; umbral de energía.

Introduction

In the study of elastic scattering of atomic nuclei at low energies there has been a long-lasting interest in the so-called threshold anomaly (TA [1]). This is an effect that becomes evident when experimental elastic scattering angular distributions, measured at several energies

around the Coulomb barrier V_c are adjusted by means of the Optical Model (OM). For the case of tightly bound nuclei, this phenomenon, is related to the closure of reaction channels at bombarding energies below the Coulomb barrier. It is manifested as a decrease of the depth of the imaginary part of the optical potential at energies below V_c . Due to the dispersion relation (DR [1]) linking

the real and imaginary parts of the optical potentials, the depth of the real part also varies strongly, peaking around V_C (see Refs. [1,2,3]), thus implying, a more attractive potential. Conversely in the case of weakly bound projectiles, the coupling to non-elastic channels (e.g. the breakup channel) generates a repulsive polarization potential [4] that can produce, either the absence of TA (no TA [5, 6, 7, 8]) or the so-called breakup threshold anomaly (BTA [7, 8, 9]), in which the imaginary potential increases while the real potential decreases in the proximity of V_C [9, 10]. In the present work new results on experimental elastic angular distributions in the ${}^9\text{Be}+{}^{80}\text{Se}$ system are presented. The data were analyzed using the OM with three different types of potentials, namely, a semi-phenomenological double folding potential with two free parameters known as the Sao Paulo Potential, a Wood-Saxon type potential with six free parameters, and an exponential potential with two free parameters. The result of this analysis is presented in section III.-Results. It will be shown in section IV.-Discussion that the three potentials yield the same results: the ${}^9\text{Be}+{}^{80}\text{Se}$ system clearly presents aBTA, independently of the potential used to reproduce the angular distributions.

Materials and methods

The elastic scattering angular distributions were measured at eleven bombarding energies: 17, 18, 19, 20, 21, 22, 23, 24, 30 and 32.8 MeV ($V_C \approx 20$ MeV). Beams of ${}^9\text{Be}$ ions were delivered by the 20 MV tandem accelerator of the TANDAR Laboratory in Buenos Aires. Enriched (99.8%) ${}^{80}\text{Se}$ targets, $110 \mu\text{g}/\text{cm}^2$ thick, evaporated onto $20 \mu\text{g}/\text{cm}^2$ thick carbon foils, were used. The detection system consisted of an array of eight surface-barrier silicon detectors with an angular separation of 5 degrees between adjacent detectors. The angular distributions were taken in angular steps from 1 to 5 degrees, depending on the energy and angular range. A second set of two surface-barrier detectors with an angular separation of 8 degrees were placed in a second rotating support at the top of the scattering chamber, to measure the reaction products at the most backward angles. The energy resolution of the detectors (FWHM) ranged from 0.5 to 0.8%, which were enough to identify and separate inelastic-excitation peaks from the elastic one. For normalization purposes two additional surface barrier detectors were placed at ± 16 degrees. The angular opening of these so-called monitor detectors, defined by circular 1.5 mm-diameter collimators, was about 0.25 degrees. Further details of the experiment are given elsewhere [11].

Results

Typical angular distributions for two energies ($E_{\text{lab}} = 18$ and 30 MeV) are shown in Figure 1. Model calculations were performed with a) a Sao Paulo potential with free N_r and N_i (normalization factors for the real and imaginary parts, respectively), b) a Wood-Saxon potential

with real part characterized with parameters V , r_0 , and a , the depth, the radius parameter and the diffusivity respectively, an imaginary part, divided in two components, a volume part with fixed parameters $V_i = 10$ MeV, $r_{i0} = 1.0$ fm and $a_i = 0.15$ fm and a variable surface part with parameters V_{si} , r_{sio} and a_{si} and c) an optical potential whose real and imaginary parts are $V = V_{10} \cdot \exp((10-R)/a)$ and $W = W_{10} \cdot \exp((10-R)/a)$ respectively, with a common rate parameter $a = 0.65$ fm. The two free parameters, V_{10} and W_{10} , represent the magnitude of the corresponding exponential functions, at an arbitrarily chosen radius, in our case 10 fm. A feature of this method is its simplicity; in this way, complex algorithms or sets of numerous and ambiguous geometric parameters are avoided.

The three potentials at $E_{\text{lab}} = 30$ MeV are compared in Figure 2. Although the three potentials are very different in the nuclear interior region they are quite similar at the nuclear surface where it is expected that most of the absorption will take place.

As indicated in the Figure 2 the results for the three potentials are shown for two energies. Very reasonable fits are obtained at all energies.

The values of the parameters for the different potentials as a function of the bombarding energy, are presented in Figure 3. The uncertainties of the parameters are obtained by means of the covariance matrix method as described in Refs. 12 and 13.

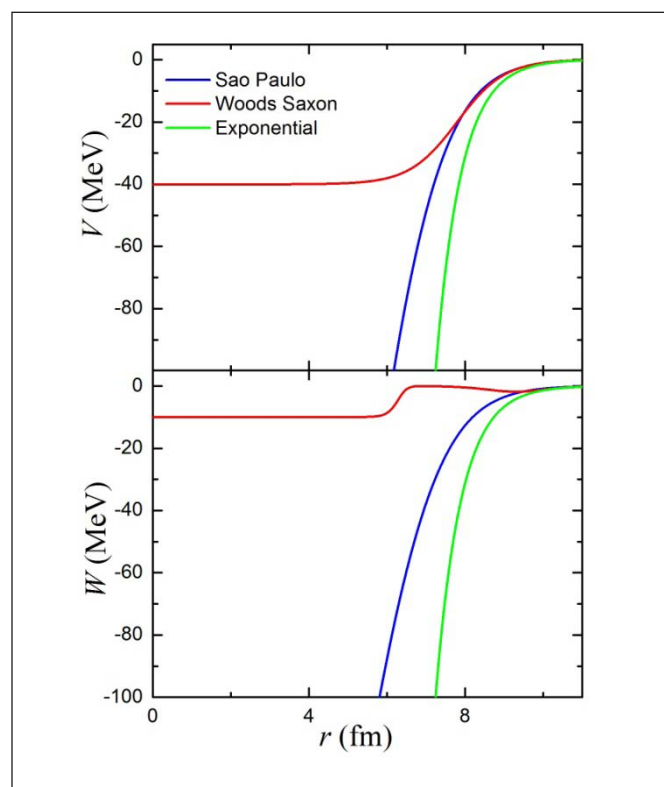


Figure 1. Real and imaginary parts of the three optical potentials discussed in the text. (For the Woods Saxon potential W represents the sum of the volume and surface components).

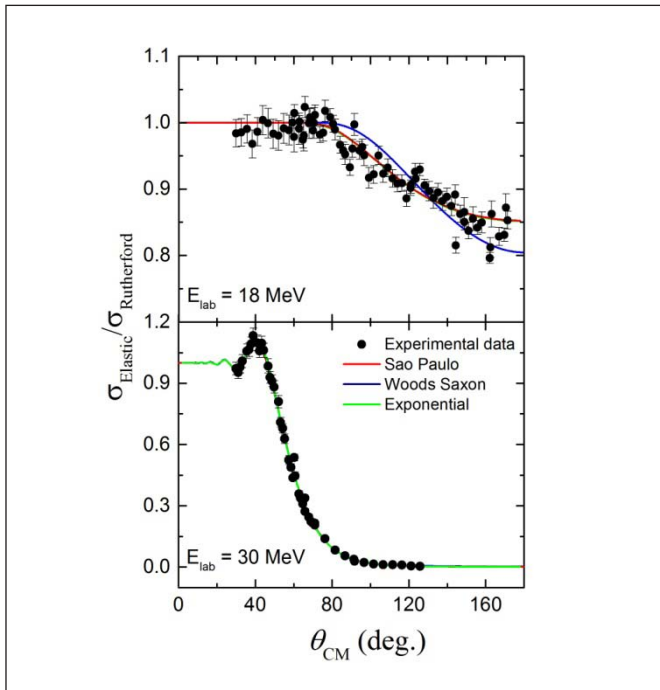


Figure 2. Elastic scattering of ${}^9\text{Be}+{}^{80}\text{Se}$ at bombarding energies of 18 and 30 MeV. Solid lines represent the optical model calculations as indicated in the figure (for $E_{\text{lab}} = 18$ MeV the curves of the Sao Paulo and the Exponential overlap, and for $E_{\text{lab}} = 30$ MeV the results are indistinguishable in the scale of the figure).

Discussion

As it was pointed out previously, three types of algorithms have been used in order to generate optical-model potentials. These potentials, as shown in Figure 1, are very different at low radial distances but quite similar over the peripheral ones, where most of the absorption takes place. Despite these circumstances, different physical quantities given by the optical model calculations are nearly coincident. First of all, the best fitted elastic differential cross-sections; some examples shown in Figure 2. They are obtained with equivalent parameters, which, of course, are different in absolute value but follow coherent behaviors as a function of the bombarding energy, as may be observed in Figure 3. As it is shown in Figure 4 for $E_{\text{lab}} = 30$ MeV, the partial reaction cross-sections are quite similar. The same may be remarked in Figure 5 for three examples of the module of the partial wave-functions; in these cases, those corresponding to the maximum orbital angular-momentum that contributes to the reaction cross-section, and those which correspond to about the half of that maximal contribution. In the case of the spatial distributions of the absorption cross-section displayed in Figure 5, the coincidences are clear for the Sao Paulo and the exponential approximations; the Woods-Saxon potential, that includes an important internal imaginary potential, leads to a shift of the internal parts of the peripheral peaks given by the two other approximations to the inner of the target, keeping their magnitude. The study of the behavior of this spatial distribution over the peripheral region at energies close to the Coulomb barrier may be useful to determine the presence of the normal or the breakup threshold anomaly.

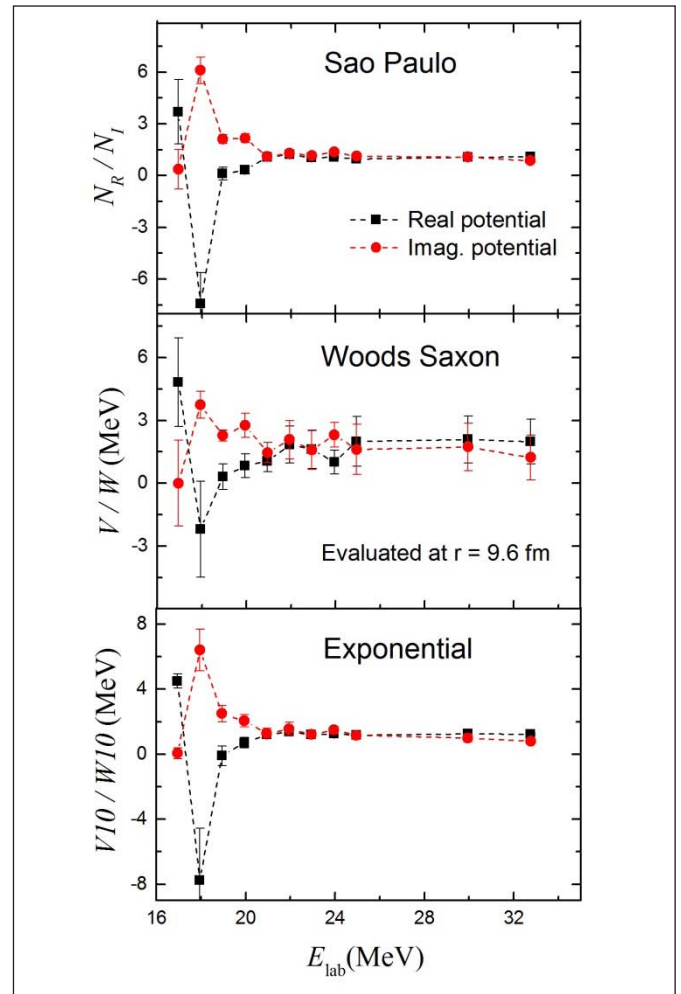


Figure 3. Energy dependence of equivalent parameters for the three potentials.

We calculate the absorption density at each radius as the sum over angular momenta L of the product of the imaginary potential W times the absolute square of the wave function Ψ .

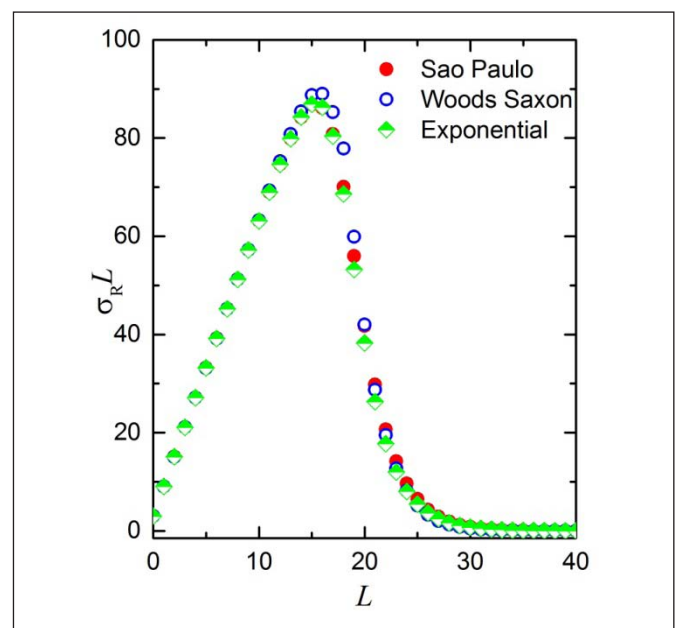


Figure 4. Partial reaction cross-sections as a function of the orbital angular momentum L for $E_{\text{lab}} = 30$ MeV. The values corresponding to each kind of potential (see text) are represented by a different symbol.

Figure 5 shows the absolute value of the partial wave functions and the partial absorption density as function of radius for the different potentials.

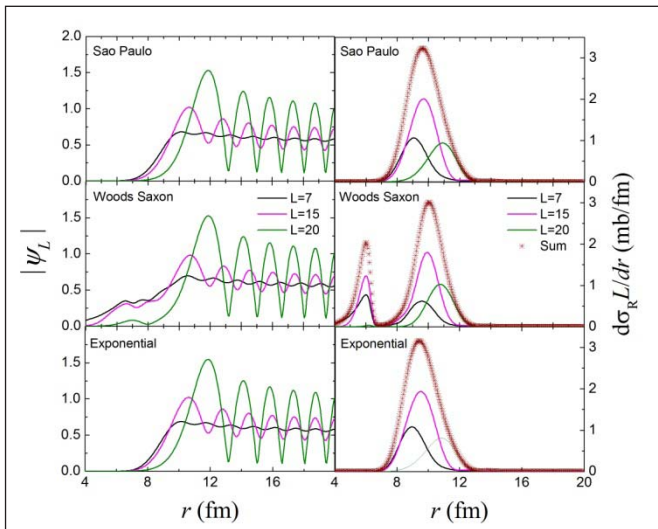


Figure 5. The partial wave-functions (left) and spatial density of absorption (right) for three significant orbital angular momenta and the different optical potential models ($E_{lab} = 30$ MeV).

Conclusions

The behavior of optical-model parameters used to describe elastic-scattering angular distributions for the ${}^9\text{Be} + {}^{80}\text{Se}$ system, which in this work are analyzed as a case study, clearly shows a breakup threshold anomaly at bombarding energies below the Coulomb barrier. This can be attributed to the low binding energy of the ${}^9\text{Be}$ projectile which favors its breakup in approaching the ${}^{80}\text{Se}$ target. It has been also shown that this conclusion is independent of the choice for the nuclear potential model. Moreover, an extremely simple model as the exponential potential, has proven to be successful in reproducing the experimental data.

References

- [1] SATCHLER GR. Heavy-ion scattering and reactions near the Coulomb barrier and “threshold anomalies”. *Phys. Rep.* 1991; 199(3): 147-190.
- [2] ABRIOLA D, DIGREGORIO D, TESTONI JE, ETCHEGOYEN A, et. al. Energy dependence of the optical potential for the ${}^{16}\text{O} + {}^{144}\text{Sm}$ system near the Coulomb barrier. *Phys. Rev. C.* 1989; 39(2): 546-552.
- [3] ABRIOLA D, SONZOGNI AA, di TADA M, ETCHEGOYEN A, et. al. Fusion and elastic scattering for the ${}^{12}\text{C} + {}^{144}\text{Sm}$ system at energies near to the Coulomb barrier. *Phys. Rev. C.* 1992; 46: 244-249.
- [4] SAKURAGI Y. Energy and target dependence of projectile breakup effect in elastic scattering of ${}^6\text{Li}$. *Phys. Rev. C.* 1987; 35(6): 2161-2174
- [5] MAHAUX C, NGO H., SATCHLER GR. Causality and the threshold anomaly of the nucleus-nucleus potential. *Nucl. Phys. A.* 1986; 449: 354-394.
- [6] KEELEY N, BENNETT SJ, CLARKE NM, FULTON BR, et. al. Optical model analyses of ${}^6,7\text{Li} + {}^{208}\text{Pb}$ elastic scattering near the Coulomb barrier. *Nucl. Phys. A.* 1994; 571(2): 326-336.
- [7] GOMES PRS, ANJOS RM, MURI C, LUBIAN J, et. al. Threshold anomaly with weakly bound projectiles: elastic scattering of ${}^9\text{Be} + {}^{27}\text{Al}$. *Phys. Rev. C.* 2004; 70(5): 054605
- [8] FIGUEIRA JM, ABRIOLA D, FERNÁNDEZ NIELLO JO, ARAZI A, et. al. Absence of the threshold anomaly in the elastic scattering of

the weakly bound projectile ${}^7\text{Li}$ on ${}^{27}\text{Al}$. *Phys. Rev. C.* 2006; 73: 054603

- [9] HUSSEIN MS, GOMES PRS, LUBIAN J, AND CHAMON LC, New manifestation of the dispersion relation: breakup threshold anomaly. *Phys. Rev. C.* 2006; 73: 044610
- [10] CANTO LF, GOMES PRS, LUBIAN J, CHAMON LC, et. al. Disentangling static and dynamic effects of low breakup threshold in fusion reactions. *Phys. Rep.* 2006; 424: 1-9.
- [11] GOLLAN F, ABRIOLA D, ARAZI A, PACHECO A, et. al. Estudio del proceso de quiebre del núcleo ${}^9\text{Be}$ en reacciones de dispersión elástica to be submitted to PRC
- [12] ABRIOLA D, ARAZI A, TESTONI JE, GOLLAN F, MARTÍ GV. Uncertainties of optical-model parameters for the study of the threshold anomaly. *J Phys: Conf Ser.* 2015; 630: 012021.
- [13] ABRIOLA D, MARTÍ GV, TESTONI JE. Bootstrap method for constructing covariance matrices of optical-model parameters in the study of the threshold anomaly. *EPJ Web of Conferences.* 2017; 146: 02050

Recibido: 13 de febrero de 2018

Aceptado: 29 de mayo de 2018